AEROELASTIC
STUDY OF A SIMPLE MODEL

—

RAYMOND L. MILLER

1956

AEROELASTIC STUDY

OF A SIMPLE MODEL

by

Lt. Raymond L. Miller USN

May 1956

AEROELASTIC STUDY OF A SIMPLE MODEL

ABSTRACT

This thesis concerns the study of a two dimensional model subjected to gust loads. The model consists of a wing attached to a fuselage of infinite moment of inertia by means of a tension-compression spring and a torsion spring.

The equations of motion were developed using two-dimensional thin airfoil theory for incompressible flow and they are solved on an electronic analogue computer. Although the equations are set up to handle a gust of any arbitrary gradient, the analysis was made for a sharp-edged gust and comparison then made with gusts of finite gradient.

It was found that stresses in the wing were reduced by locating the center of gravity near the elastic center and by reducing the radius of gyration of the wing. There were two oscillatory modes, one primarily bending and the other primarily torsion. The frequencies of oscillation could be lowered by locating the center of gravity near the elastic center, by increasing the radius of gyration or by increasing the wing to fuselage mass ratio.

The mode primarily characterized by torsion had a relatively high frequency at low flight velocity. The two frequencies approached each other as flight velocity increased and damping was improved in each mode until flutter was imminent, when the lower frequency (bending) mode very suddenly became unstable. It was found that neglecting the unsteady effects yielded a highly conservative estimate of flutter speed in this particular case.

Increase in altitude has little effect but to lessen the damping in each mode.

AEROELASTIC STUDY OF A SIMPLE MODEL

INTRODUCTION

The purpose of the present thesis was the investigation of the response to gust loads of a two-dimensional model with three degrees of freedom; particularly, the effect upon such response of changes in environmental and model parameters.

The present thesis was submitted at the University of Michigan in partial fulfillment of the requirements for the degree of Master of Science in Aeronautical Engineering. The subject was suggested by Associate Professor Gabriel Isakson of the Aeronautical Engineering Department and performed under his supervision. The approach to the problem was patterned after an earlier report by Professor Isakson (Ref. 1), but, with solution of the equations performed by means of electronic analogue computers, rather than analytically.

The problem to be investigated is that of aeroelastic effects on a two-dimensional wing-fuselage combination in incompressible flow. The wing has freedom in twist and bending; the fuselage is free to plunge vertically, but is restrained in pitch.

THEORY

1. The Problem

The two-dimensional model consists of a fuselage and thin wing of constant cross section connected by a tension-compression spring and a torsion spring, representing the elastic constraints of the wing in bending and torsion respectively, as shown in Figure 1. Z_w and Z_f are vertical displacements of the wing and fuselage respectively, relative to fixed axes, and θ is the rotation of the wing chord about the elastic center. All are positive in the directions shown and are measured from the initial steady state position.
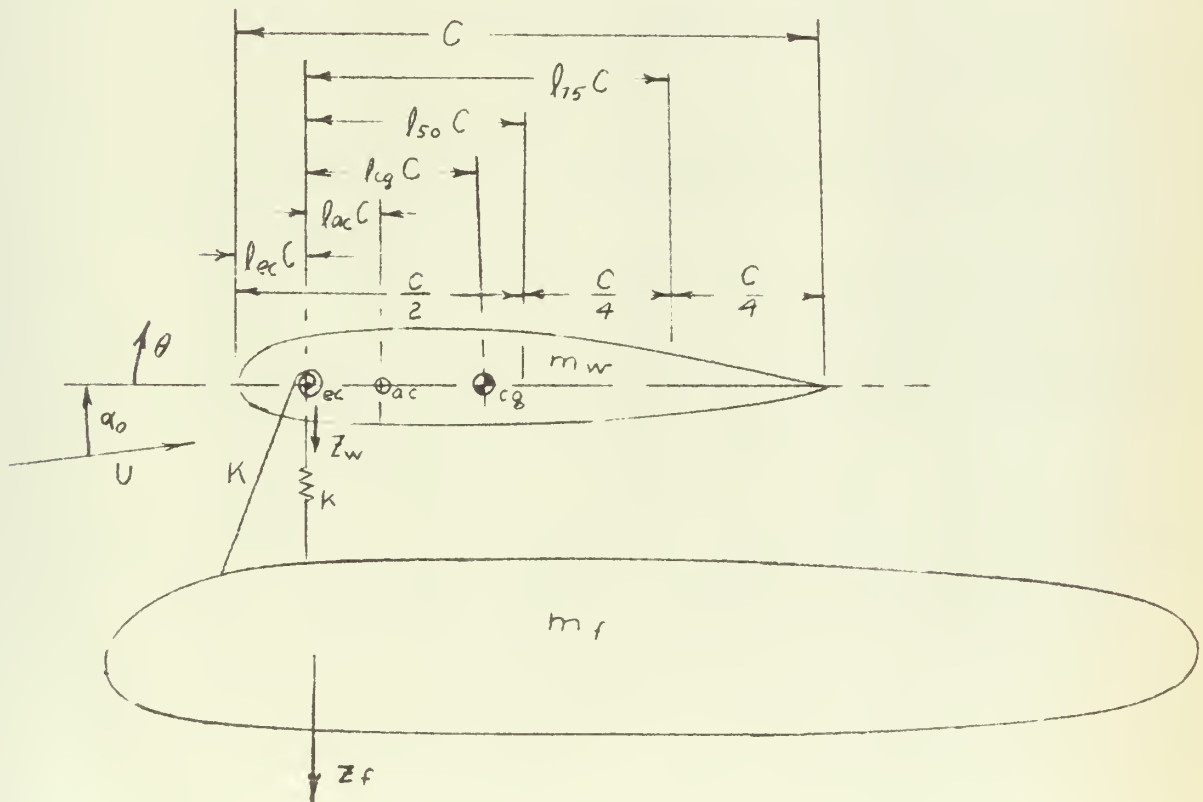

Fig. 1

The angles α_o, θ and the changes in angle of attack due to gusts and due to vertical velocity of the wing $\dot{Z}_w$ are assumed to be small and the cosines of these angles are taken to be unity in evaluating aerodynamic lift and moment. The gust acting upon the model is taken to be normal to the velocity vector, U, of the undisturbed free stream.

2. The Equations of Motion

The equations of motion of the system are:

$$m_w \ddot{Z}_w + R \ddot{\theta} + k(Z_w - Z_f) = -L \tag{1}$$

$$R \ddot{Z}_w + I \ddot{\theta} + K \theta = M \tag{2}$$

$$m_f \ddot{Z}_f - k(Z_w - Z_f) = 0 \tag{3}$$

where:

k = spring constant of tension-compression spring.

K = spring constant of torsion spring.

I = mass moment of inertia of airfoil section about the elastic center.

   = $I_{cg} + m_w(l_{cg}C)^2$

I_{cg} = mass moment of inertia of airfoil section about the center of gravity.

L = instantaneous value of aerodynamic lift per unit span, as a departure from the initial steady state value, positive up.

M = instantaneous value of aerodynamic moment per unit span, as a departure from the initial steady state value, positive in the direction of θ.

m_f = mass of fuselage per unit span

m_w = mass of wing per unit span

R = static mass moment about the elastic center.

   = $m_w(l_{cg}C)$

It is convenient to change from a time variable, t, to a variable, s, where:

$$s = \bar{U}_t = \text{distance travelled in half-chords.}$$

$$\bar{U} = U\frac{2}{C} = \text{velocity of flight in half-chords per unit of time.}$$

Under this transformation:

$$\frac{d}{dt} = \bar{U}\frac{d}{ds}$$

$$\frac{d^2}{dt^2} = \bar{U}^2\frac{d^2}{ds^2}$$

Denoting differentiation with respect to s by prime marks:

$$m_w\bar{U}^2 Z_w'' + R\bar{U}^2\theta'' + k(Z_w - Z_f) = -L(s) \tag{4}$$

$$R\bar{U}^2 Z_w'' + I\bar{U}^2\theta'' + K\theta = M(s) \tag{5}$$

$$m_f\bar{U}^2 Z_f'' - k(Z_w - Z_f) = 0 \tag{6}$$

These equations are now put in non-dimensional form:

$$\frac{Z_w''}{C} + l_{cg}\theta'' + K_B(\frac{Z_w}{C} - \frac{Z_f}{C}) = -\frac{L}{m_w\bar{U}^2 C} \tag{7}$$

$$l_{cg}\frac{Z_w''}{C} + r^2\theta'' + K_T\theta = \frac{M}{m_w\bar{U}^2 C^2} \tag{8}$$

$$\frac{m_f}{m_w}\frac{Z_f''}{C} - K_B(\frac{Z_w}{C} - \frac{Z_f}{C}) = 0 \tag{9}$$

where:

$$r = \frac{1}{C}\sqrt{\frac{I}{m_w}} = \text{radius of gyration as a fraction of the chord}$$

$$K_B = \frac{k}{m_w\bar{U}^2} = \frac{kC^2}{4m_wU^2} = \text{bending stiffness parameter}$$

$$K_T = \frac{K}{m_w\bar{U}^2 C^2} = \frac{K}{4m_wU^2} = \text{torsion stiffness parameter}$$

3. Aerodynamic Force and Moment

Four types of force and moment act on the airfoil as a departure from initial steady state values:

1) Gust effect

2) Wake effect

3) "Quasi-steady" forces - forces which would be produced by the instantaneous velocity of the airfoil in the absence of wake effect.

4) Apparent mass effect

The last three forces listed are results of the disturbed motion of the airfoil. The quasi-steady forces and the wake effect can be accounted for simultaneously; thus, lift and moment each consist of three components:

$$L = L_g + L_m + L_{ma} \qquad (10)$$

$$M = M_g + M_m + M_{ma} \qquad (11)$$

L_g = lift due to gust effect.

L_m = lift due to quasi-steady forces and wake effect resulting from airfoil motion.

L_{ma} = lift due to apparent mass effect.

M_g = moment due to gust effect.

M_m = moment due to quasi-steady forces and wake effect resulting from airfoil motion.

M_{ma} = moment due to apparent mass effect.

Lift and moment are computed by thin airfoil theory.

3.1. Gust effect

For sharp-edged gusts, the change in lift coefficient is a function of time (or distance in half-chords):

$$C_L = \frac{dC_L}{d\alpha} \Delta \alpha \psi(s) = 2\pi \frac{w}{U} \psi(s)$$

where w is the gust velocity, positive up, and $\psi(s)$ is the Küssner function for build-up of lift due to change of angle of attack in a sharp-edged gust, the value of this function approaching unity with increase is s.

A gust of arbitrary gradient can be considered to be made up of a series of infinitesimal sharp-edged gusts as shown in Fig. 2. The lift coefficient can be computed for each infinitesimal gust by the formula above and all the values summed by integration. Thus the change of lift coefficient becomes a function

Fig. 2

of (s - σ), where σ is the value of s at the time of origin of the particular infinitesimal gust (Δw):

$$C_L = \frac{2\pi}{U} \Delta w \, \psi(s - \sigma)$$

Summing the effects of all the infinitesimal gusts:

$$C_L = \frac{2\pi}{U} \left\{ w(o) \, \psi(s) + \sum_{\sigma = \Delta\sigma}^{s} \Delta w(\sigma) \psi(s - \sigma) \right\}$$

$$C_L = \frac{2\pi}{U} \left\{ w(o)\, \psi(s) + \sum_{\sigma=\Delta\sigma}^{s} \frac{\Delta w(\sigma)}{\Delta\sigma} \psi(s-\sigma)\, \Delta\sigma \right\}$$

or, in the limit as $\Delta\sigma \to 0$:

$$C_L = \frac{2\pi}{U} \left\{ w(o)\, \psi(s) + \int_0^s w'(\sigma)\, \psi(s-\sigma)\, d\sigma \right\} \tag{12}$$

This is the Duhamel, or superposition, integral. An equivalent form is found by integration by parts:

$$C_L = \frac{2\pi}{U} \left\{ w(s)\, \psi(o) + \int_0^s w(\sigma)\, \psi'(s-\sigma)\, d\sigma \right\} \tag{13}$$

It will be shown later that $\psi(0) = 0$, thus:

$$C_L = 2\pi \int_0^s \frac{w(\sigma)}{U} \psi'(s-\sigma)\, d\sigma$$

$$L_g = \frac{\rho}{2} C U^2 C_L = \frac{\rho}{8} c^3 \bar{U}^2 C_L$$

$$L_g(s) = \frac{\pi\rho}{4} \bar{U}^2 c^3 \int_0^s \frac{w}{U}(\sigma)\, \psi'(s-\sigma) d\sigma \tag{14}$$

In two-dimensional thin airfoil theory for incompressible flow, the aerodynamic center is at the 25% chord point:

$$l_{ac} = l_{25}$$

$$M_g(s) = -(l_{ac}C)\, L_g(s) \tag{15}$$

3.2 Quasi-Steady Forces and Wake Effect

The sum of the quasi-steady forces and wake effect is a function not only of the instantaneous disturbed motion of the airfoil, but also of the time history of that motion. These forces build up with time in much the same fashion as change in forces due to a gust and are handled in similar fashion. It can be shown that the terms which are functions of the time history of the disturbed

motion are all related to the quantity:

$$(\dot{Z}_w + U\theta + l_{75} C\dot{\theta})$$

(Ref. 2, page 282). This quantity can be seen to be the instantaneous vertical velocity of the three-quarter chord point and is equal to the angle of attack at that point times the flight velocity, U. Thus, by resolving velocities at the three-quarter chord point, the quasi-steady forces and wake effect can be accounted for simultaneously The lift due to these forces can be found by a process analogous to that due to the gust effect:

$$L_m = \frac{\pi \rho}{4} \, \bar{U}^2 C^3 \int_0^S \phi \, (s - \sigma) \alpha'_{75} (\sigma) \, d\sigma \tag{16}$$

where:

$$\alpha_{75}(t) = \theta(t) + \frac{l_{75}C}{U} \dot{\theta}(t) + \frac{1}{U} \dot{Z}_w(t)$$

$$\alpha_{75}(s) = \theta(s) + 2l_{75} \theta'(s) + 2\frac{Z'_w}{C} \tag{17}$$

α_{75} is the angle of attack at the three-quarter chord point, measured as a departure from the initial steady state value, and $\phi(s)$ is the Wagner function for build up of lift coefficient following a sudden change of angle of attack. Like the Küssner function, the Wagner function is defined to approach unity with increasing s.

The above equation is a form of the Duhamel integral as in equation (12), but with $\alpha_{75}(0) = 0$.

The lift due to the quasi-steady forces and the wake effect acts at the 25% chord point, except for that part of the quasi-steady lift, equal to $\pi \rho (\frac{C}{2})^2 (U\dot{\theta})$, which is due to the rotational velocity of the airfoil and acts at the 50% chord point (Ref. 3, page 104). This, then, must be subtracted from the moment:

$$\frac{C}{4} \times \pi\rho(\frac{C}{2})^2 \ \frac{\bar{U}^2 C}{2} \theta'(s) = \frac{\pi\rho}{32} \bar{U}^2 C^4 \theta'(s)$$

$$M_m(s) = -l_{ac} L_m - \frac{\pi\rho}{32} \bar{U}^2 C^4 \theta'(s) \tag{18}$$

3.3. Apparent Mass

The apparent mass lift due to the disturbed motion of the airfoil may be thought of as the force associated with the acceleration of a cylinder of air with diameter equal to the wing chord. It is equal to the product of $\pi\rho(\frac{C}{2})^2$ and the instantaneous acceleration of the 50% chord point. In addition a pure couple is acting on the airfoil equal to the product of $-\frac{\pi\rho}{8}(\frac{C}{2})^4$ and the instantaneous rotational acceleration of the airfoil (Ref. 2, page 263).

The distrubed velocity of the 50% chord point relative to the free stream is:

$$\dot{Z}_w + U\theta + l_{50} C \dot{\theta}$$

and the acceleration of the point is:

$$\ddot{Z}_w + U\dot{\theta} + l_{50} C \ddot{\theta}$$

Thus;

$$L_{ma} = \frac{\pi\rho}{4} C^2 (\ddot{Z}_w + U\dot{\theta} + l_{50} C \ddot{\theta})$$

$$= \frac{\pi\rho}{4} \bar{U}^2 C^3 (\frac{Z_w''}{C} + \frac{1}{2}\theta' + l_{50}\theta'') \tag{19}$$

$$M_{ma} = -l_{50} C L_{ma} - \frac{\pi\rho}{8} \frac{C^4}{16} \ddot{\theta}$$

$$= -l_{ac} C L_{ma} - \frac{\pi\rho}{16} \bar{U}^2 C^4 \left\{ \frac{Z_w''}{C} + \frac{1}{2}\theta' + (l_{50} + \frac{1}{8})\theta'' \right\} \tag{20}$$

summing equations 14, 16, 19 and 15, 18, 20 for total lift and moment:

$$L(s) = \frac{\pi \rho}{4} \bar{U}^2 C^3 \left\{ \int_0^s \frac{w}{U}(\sigma) \, \psi'(s-\sigma) \, d\sigma + \int_0^s \phi(s-\sigma) \alpha'_{75}(\sigma) \, d\sigma \right.$$

$$\left. + \left(\frac{Z''}{C} + \frac{1}{2} \theta' + l_{50} \theta'' \right) \right. \tag{21}$$

$$M(s) = -l_{ac} C \, L(s) - \frac{\pi \rho}{16} \bar{U}^2 C^4 \left\{ \frac{Z''}{C} + \theta' + \left(l_{50} + \frac{1}{8} \right) \theta'' \right\} \tag{22}$$

Dividing equation (21) by $m_w \bar{U}^2 C$ and equation (22) by $m_w \bar{U}^2 C^2$:

$$\frac{L(s)}{m_w \bar{U}^2 C} = \frac{1}{\mu} \left\{ \int_0^s \left(\frac{w}{U} \right)(\sigma) \psi'(s-\sigma) d\sigma + \int_0^s \phi(s-\sigma) \alpha'_{75}(\sigma) \, d\sigma \right.$$

$$\left. + \left(\frac{Z''_w}{C} + \frac{1}{2} \theta' + l_{50} \theta'' \right) \right\} \tag{23}$$

$$\frac{M(s)}{m_w \bar{U}^2 C^2} = - \frac{l_{ac} L(s)}{m_w \bar{U}^2 C} - \frac{1}{4\mu} \left\{ \frac{Z''_w}{C} + \theta' + \left(l_{50} + \frac{1}{8} \right) \theta'' \right\}$$

$$= - \frac{l_{ac}}{\mu} \left\{ \int_0^s \frac{w}{U}(\sigma) \psi'(s-\sigma) \, d\sigma + \int_0^s \phi(s-\sigma) \alpha'_{75}(\sigma) d\sigma \right\}$$

$$- \frac{1}{\mu} \left\{ l_{50} \frac{Z''_w}{C} + \frac{l_{75}}{2} \theta' + \left(l_{50}^2 + \frac{1}{32} \right) \theta'' \right\} \tag{24}$$

where:

$$\mu = \frac{m_w}{\pi \left(\frac{C}{2} \right)^2 \rho} = \text{relative density}$$

= ratio of mass of wing to mass of a cylinder of air with

diameter equal to wing chord.

Now these expressions for lift and moment can be substituted into the equations

of motion, (7) and (8):

$$(1 + \frac{1}{\mu}) \frac{Z_w}{C} + (l_{cg} + \frac{l_{so}}{\mu}) \theta'' + \frac{1}{2\mu} \theta' + K_B (\frac{Z_w}{C} - \frac{Z_f}{C})$$
$$+ \frac{1}{\mu} \left\{ \int_0^s \frac{w}{U}(\sigma) \psi'(s-\sigma) d\sigma + \int_0^s \phi(s-\sigma) \alpha'_{1s}(\sigma) d\sigma \right\} = 0 \qquad (25)$$

$$(r^2 + \frac{l_{so}^2 + \frac{1}{32}}{\mu}) \theta'' + (l_{cg} + \frac{l_{so}}{\mu}) \frac{Z}{C}'' + \frac{l_{7s}}{2\mu} \theta' + K_T \theta$$
$$+ \frac{l_{9s}}{\mu} \left\{ \int_0^s \frac{w}{U}(\sigma) \psi'(s-\sigma) d\sigma + \int_0^s \phi(s-\sigma) \alpha'_{7s}(\sigma) d\sigma \right\} = 0 \qquad (26)$$

4. Wagner and Küssner functions

The exact forms of the Wagner and Küssner functions for incompressible

flow involve Bessel functions (Ref. 2, page 285, 287):

$$\phi(s) = \frac{2}{\pi} \int_0^\infty \frac{F(k)}{k} \sin ks \, dk = 1 + \frac{2}{\pi} \int_0^\infty \frac{G(k)}{k} \cos ks \, dk$$

$$\psi(s) = \frac{2}{\pi} \int_0^\infty \frac{\left[F_G(k) - G_G(k)\right] \sin ks \sin k}{k} \, dk$$

where:

$$F(k) + i G(k) = C(k) = \frac{H_1^{(2)}(k)}{H_1^{(2)}(k) + i H_0^{(2)}(k)}$$

$$H_n^{(2)} = J_n - i Y_n$$

$$F_G(k) + i G_G(k) = C(k) \left[J_o(k) - i J_1(k) \right] + i J_1(k)$$

J_n = Bessel function of the first kind of order n

Y_n = Bessel function of the second kind of order n

Since these functions are too complex for analytical use, it is necessary to use

the following approximations:

$$\phi(s) = 1 - 0.165 e^{-0.0455s} - 0.335 e^{-0.35} \qquad (27)$$

$$\psi(s) = 1 - 0.500 e^{-0.130s} - 0.500 e^{-s} \qquad (28)$$

These equations show that a sudden change in angle of attack due to an instan-

taneous disturbed motion of the airfoil immediately causes a change in lift

coefficient then increases asymptotically to the ultimate steady state value;

whereas, a sharp-edged gust causes no initial change in lift coefficient, but then causes the lift coefficient to increase asymptotically to its ultimate steady state value.

Using the approximate equations, (27) and (28), for the Wagner and Küssner functions, the equations of motion can be solved, either analytically or by means of the analogue computer.

5. Dynamic Overstress Factors

The dynamic overstress factor is defined as the ratio of the maximum stress the wing of the elastic model is subjected to by a given gust to the maximum stress the corresponding rigid model ($K_T = K_B = o$) would be subjected to by the same gust.

Dynamic overstress factor in bending

$$
= \frac{K \left(\dfrac{Z_w}{C} - \dfrac{Z_f}{C}\right) \text{ elastic}}{K \left(\dfrac{Z_w}{C} - \dfrac{Z_f}{C}\right) \text{ rigid}} = \frac{(Z_f'') \text{ elastic}}{(Z_f'') \text{ rigid}}
$$

Dynamic overstress factor in torsion

$$
= \frac{(K\,\theta) \text{ elastic}}{(K\,\theta) \text{ rigid}}
$$

From equations (8) and (24):

$$
(K_T\,\theta) \text{ rigid} = \frac{M}{M_w \bar{U}^2 C^2} - l_{cg} \frac{Z_w''}{C}
$$

$$
\frac{M}{M_w \bar{U}^2 C^2} = -\frac{l_{ac}}{\mu} \left\{ \int_0^s \frac{w}{U}(\sigma) \psi'(s-\sigma)d\sigma + \int_0^s \phi(s-\sigma)\alpha_{75}(\sigma)\,d\sigma \right\}
$$

$$
-\frac{l_{50}}{\mu} \frac{Z_w''}{C}
$$

thus;

$$(K_T \, \theta) \, \text{rigid} \; = \; - \, \frac{l_{ac}}{\mu} \, \left\{ \int_0^s \frac{w}{U} (\sigma) \psi'(s - \sigma) d\sigma \; + \; \int_0^s \phi (s - \sigma) \alpha'_{75}(\sigma) d\sigma \right\}$$

$$- \; (\frac{l_{50}}{\mu} + l_{cg}) \frac{Z''_w}{C} \qquad (29)$$

PROCEDURE

Representative values of the various parameters were selected to serve
as a standard or basis of comparison in observing gust and flutter effects. The
standard values of these parameters were selected arbitrarily, but were intended
to represent a transport or trainer type of aircraft. Standard values and range
considered are shown in Table I.

The stiffness parameters, K_B and K_T, were selected to correspond to un-
coupled frequencies of approximately 200 cycles per minute in bending and 475
cycles per minute in torsion:

$$K_B \; = \; \frac{k}{m_w} \, \frac{C^2}{4U^2} \; = \omega_B^2 \; \frac{C^2}{4U^2}$$

$$K_T \; = \; \frac{K}{m_w} \, \frac{C}{4U^2} \; = \omega_T^2 \; \frac{C}{4U^2}$$

$$\omega_B \; = \; \frac{2U}{C} \, \sqrt{K_B} \; = \; 193 \; \text{cycles/min.}$$

$$\omega_T \; = \; \frac{2U}{C^2} \sqrt{K_T} \; = \; 470 \; \text{cycles/min.}$$

The effects of individual model parameters were investigated while holding
all other parameters fixed. Similarly, the effect of altitude and flight velocity
were investigated. Dynamic overstress factors were determined by measuring

the maximum acceleration of the fuselage and twist of the wing under a step input representing a sharp-edge gust. The period, damping time and mode shape of each of the oscillatory modes were determined by adjusting initial conditions to separate the modes.

<div align="center">ELECTRONIC CIRCUITS</div>

1. General

The computer primarily used for solution of the problem was a Reeves Electronic Analogue Computer (REAC Mod. C 101). Traces were made on a Brush Oscillograph recorder (Model BL-928) using a Brush Dual Channel D-C Amplifier (Model BL-202).

The complete circuit diagrams are shown in Figs. 5 and 6.

2. Scaling

It was found convenient to speed up the solution by scaling. Under the transformation, $s_1 = .2s$, the equations become:

$$\frac{Z''_f}{C} = 25 K_B \frac{m_w}{m_f} \left(\frac{Z_w}{C} - \frac{Z_f}{C} \right) \tag{30}$$

$$\alpha_{75} = \theta + .41_{75} \theta' + .4\frac{Z'_w}{C} \tag{31}$$

$$\frac{Z''_w}{C} = -\left(\frac{l_{cg}\mu + l_{50}}{\mu + 1}\right)\theta'' - \frac{2.5}{\mu + 1}\theta' - \frac{25K_B}{\mu + 1}\left(\frac{Z_w}{C} - \frac{Z_f}{C}\right)$$

$$- \frac{25}{\mu + 1}\left\{ \int_o^{S_1} \frac{\ddot{w}}{U}(\sigma)\psi'(s - \sigma)d\sigma + \int_o^{S_1} \ddot{\phi}(s - \sigma)\alpha'_{75}(\sigma)\,d\sigma \right\} \tag{32}$$

$$(r^2\mu + 1^2_{50} + \frac{1}{32})\theta'' = -(l_{cg}\mu + l_{50})\frac{Z''_w}{C} - 2.5]_{75}\theta'$$

$$-25K_T\mu\theta - 25L_{ac}\left\{ \int_o^{S_1} \frac{\ddot{w}}{U}(\sigma)\psi'(s - \sigma)d\sigma + \int_o^{S_1} \ddot{\phi}(s_1 - \sigma)\alpha_{75}(\sigma)\,d\sigma \right\} \tag{33}$$

$$\phi(s_1) = 1 - 0.165\,e^{-0.2275\,s_1} - 0.335\,e^{-1.5\,s_1} \tag{34}$$

$$\psi(s_1) = 1 - 0.500\,e^{-5\,s_1} - 0.500\,e^{-0.65\,s_1} \tag{35}$$

$$(K_T\,\theta)\ \text{rigid} = -\left(\frac{l_{cg} + l_{50}/\mu}{25}\right)\frac{Z'w}{C} - \frac{l_{ac}}{\mu}\left\{\int_0^{s_1}\frac{w}{U}(\sigma)\,\psi'(s-\sigma)\,d\sigma\right.$$

$$\left. + \int_0^{s_1}\phi(s-\sigma)\,\alpha'_{75}(\sigma)\,d\sigma\right\} \tag{36}$$

3. Symbols

4. Convolution Integrals

The analytic solution of the convolution integrals requires an integration for each exponential term; similarly the computer solution requires an integrator for each exponential term. Consider the following circuit:

The differential equation for this circuit is:

$$\frac{dx}{dt} + ax = -AN(t)$$

and the solution is:

$$x = -Ae^{-at} \int e^{at} N(t)dt$$

$$= -Ae^{-at} \int_0^t e^{a\tau}N(\tau)\,d\tau$$

$$= -A \int_0^t e^{-a(t-\tau)}N(\tau)d\tau$$

Thus the Küssner function can be developed by the circuit shown in Fig. 3.

Fig. 3. Küssner Function Circuit

It is possible, by the use of an external circuit, to develop the convolution integral with only one amplifier. In order to conserve integrators, the Wagner function was handled in such a manner.

The above circuit can be shown to satisfy the differential equation:

$$e'_o + \frac{1}{CR_i} e_o = - \frac{R_f}{R_i} e'_i$$

and its solution is:

$$e_o = - \frac{R_f}{R_i} \int_0^t e^{- \frac{1}{CR_i}(t-\tau)} e'_i(\tau) d\tau$$

and, by the use of helipots, more than one exponential can be handled with a single amplifier:

where:

$$e_o = - A \frac{R_f}{R_1} \int_0^t e^{-\frac{1}{C_1 R_1}(t-\tau)} e'_i(\tau)d\tau - B \frac{R_f}{R_2} \int_0^t e^{-\frac{1}{C_2 R_2}(t-\tau)} e'_i(\tau)d\tau$$

The circuit for the Wagner function is as shown in Fig. 4.

Fig. 4. Wagner Function Circuit

RESULTS AND DISCUSSION

1. Accuracy of data

The accuracy in measurement of amplitudes was less limited by the computer than by the recorder, which was accurate within about 4%. This produced good results in determination of dynamic overstresses and smooth curves were obtained in all cases. Determination of mode shapes was quite difficult, not primarily due to any inherent inaccuracy in the computer, but due to the difficulty encountered in obtaining the modes in pure form; by averaging over several cycles, consistent values were obtained in most cases. (Mode shapes were measured in bending and torsion amplitudes only, phase angle changes were too small to be measured except near flutter speed.) The same difficulty was encountered measuring the damping of the oscillatory modes and the averaging procedures were somewhat less successful.

2. Behavior of the Model in the Standard Configuration

In the standard configuration the elastic center is .35 chord lengths from the leading edge, the center of gravity is .45 chord lengths from the leading edge, the radius of gyration is equal to .25 chord lengths and the wing to fuselage mass ratio is .333; the model has a relative density of 50 at sea level with a flight velocity of 380 feet per second. The model experiences dynamic overstress factors of 1.90 in bending and 2.35 in torsion under the action of a sharp-edged gust. There are two oscillatory modes, one primarily involving bending and the other primarily involving torsion. The "bending" mode has a frequency of 222 cycles per minute and damps to one-half amplitude in 3.7 cycles. The torsion mode has a frequency of 589 cycles per minute and damps to one half amplitude

in 5.7 cycles. The mode shapes are:

$$\left(\frac{Z_w - Z_f}{\theta}\right)_{bending} = 3.69 \text{ chord lengths/radian}$$

$$\left(\frac{Z_w - Z_f}{\theta}\right)_{torsion} = -0.108 \text{ chord lengths/radian}$$

where the minus sign indicates that the bending and torsional displacements are approximately $180°$ out of phase.

3. Effect of the Location of the Elastic Center and Center of Gravity

The effect of the elastic center and center of gravity locations on the dynamic overstress factors under the action of a sharp-edged gust is shown in Fig. 7; neither has any appreciable effect on the dynamic overstress in bending; however, the dynamic overstress in torsion increases as the elastic center and the center of gravity move apart.

Effects of the elastic center and center of gravity location upon frequencies, damping and mode shapes are shown in Figs. 8-10; in interpreting these curves, it should be remembered that the elastic center is initially at the .35 chord point and the center of gravity at the .45 chord point and each parameter is adjusted individually, not simultaneously. Fig. 8 shows that the frequency of the torsion mode is at a minimum when the elastic center is coincident with the center of gravity and increases rapidly as the elastic center moves ahead of the center of gravity. The frequency of the bending mode is little affected by the elastic center or center of gravity location and is not shown in Fig. 8.

The damping constants obtained in investigating the effect of varying the elastic center location were somewhat erratic, but it is apparent from Fig. 9 that the damping of the torsional mode decreases as the center of gravity moves

aft and as the elastic center moves toward the center of gravity. The damping of the bending mode is a minimum when the center of gravity is located near the .35 chord point, although the effect on damping of either center of gravity or elastic center location is quite small.

As seen in Fig. 10, the bending mode is free from any influence of torsion when the center of gravity is located just slightly ahead of the elastic center, and the torsion mode is free from any influence of bending when the elastic center is just slightly ahead of the center of gravity. The slight coupling that occurs when the elastic center and center of gravity are coincident is due to the apparent mass aerodynamic effect.

4. Effect of the Radius of Gyration

Effect of the radius of gyration on dynamic overstress factors and mode characteristics is plotted in Figs. 11-12. The dynamic overstress factor in torsion increases as the radius of gyration increases. This is consistent with increases in dynamic overstress factor as the elastic center and center of gravity move apart.

Again in this case, the damping constants were somewhat erratic, but damping of the torsion mode was seen to improve as the radius of gyration decreased; the frequency of the torsion mode increases as the radius of gyration decreases. The influence of torsion in the bending mode increases as the radius of gyration becomes smaller. The frequency and damping of the bending mode and the mode shape of the torsion mode are little affected by the radius of gyration and these effects are not shown in Fig. 12.

5. Effect of Wing to Fuselage Mass Ratio

The effect of changing the fuselage mass, while holding the wing mass fixed

is shown in Figs. 13-15. The dynamic overstress factors are increased some-
what as the mass ratio, m_w/m_f, is increased. The frequency of the bending
mode increases and the damping decreases as the fuselage becomes lighter.
The frequency and damping of the torsion mode is not noticeably affected and is
not shown. Coupling between the two modes is at a minimum at a mass ratio of
about .30.

6. Effect of Flight Velocity

The effects of flight velocity on behavior of the model are shown in Figs. 16-
18. The flutter speed for the model was found to be 1142 feet per second (com-
pressibility effects neglected). As the flutter speed is approached the frequencies
of the two modes approach each other as would be expected (Ref. 4, page 222)
and the damping improves in each mode until very near the flutter speed, where
the damping of the bending mode drops off sharply. This sudden deterioration of
damping also might be expected; a study of a three dimensional wing of large
aspect ratio produced frequency and damping characteristics very similar to
those of Fig. 17 (Ref. 2, pages 552-3). Torsion becomes more predominant in
each mode with increase in speed.

The dynamic overstresses increase gradually at first with increase in flight
velocity, and then rise sharply at the flutter speed; this is especially true of the
dynamic overstress in torsion.

7. Effect of Altitude

Figs. 19-20 show the effect of altitude or relative density on dynamic over-
stress factors and damping. As the altitude is increased above sea level (or
density reduced), it was found that frequencies of the modes are not discernably
changed, nor are the mode shapes significantly affected; thus frequencies and
mode shapes are not plotted. The damping is decreased in both modes; this

decrease in damping does not mean that the flutter speed would be reduced; in fact, it is shown in Ref. 2 (page 542) by analysis of an airfoil model with freedom in bending and torsion, that increase in the relative density (above a fairly small figure) increases the flutter speed. This is logical since damping is improved with increased airspeed. Dynamic overstress factors are not greatly affected by the value of the relative density, except for values of relative density approaching zero.

8. Neglect of Unsteady Forces

Substitution of quasi-steady forces for the unsteady forces is accomplished by replacing the Wagner function with unity; this gives a slightly conservative estimate of dynamic overstresses and a very conservative estimate of flutter speed - 498 ft/sec. as compared to 1142 ft/sec. It is of interest, however, that flutter occurs in the torsion mode, not in the bending mode as with the unsteady forces included. An analysis of a jet transport wing (Ref. 2, pages 567-8) produced similar results, except that flutter occurs in the torsion mode for both unsteady and quasi-steady theory.

On the basis of a constant derivative analysis, in order for energy to be extracted from the air the following criterion must be met.

$$\frac{\omega C}{U} < 1.56$$

(Ref. 5, page 64). Flutter of this model under quasi-steady analysis occurs at a frequency of 58.7 radians per second; i.e.:

$$\frac{\omega C}{U} = 1.40$$

9. Gust Gradient

A gust with a finite gradient would cause lower stresses on the wing than

a sharp-edged gust. Fig. 21 shows the effect on the stresses as function of time required for the gust to build up to its maximum value.

CONCLUSIONS

It was found that, for this two-dimensional model, dynamic overstresses caused by a sharp-edged gust could be reduced by locating the center of gravity close to the elastic center or by reducing the radius of gyration of the wing. The frequencies of the oscillatory modes were increased by locating the center of gravity near the elastic center, by increasing the radius of gyration or by increasing the wing to fuselage mass ratio. Damping of the torsion model is best when the center of gravity and elastic center are coincident, but damping of the bending mode is improved by moving the center of gravity and elastic center apart - also by decreasing the wing to fuselage mass ratio.

As flight velocity increases the dynamic overstresses increase and the two oscillatory modes approach each other in frequency; each mode becoming more highly damped until one of the modes very suddenly becomes unstable and flutter occurs. Neglecting the unsteady forces yields a highly conservative estimate of flutter speed in the present case.

Increasing altitude at constant velocity decreases the damping in each mode.

This study has been concerned with changes in only one parameter at a time. Further study might well be done on the interactions of two or more parameters: for example, the influence of the various parameters on flutter speed. Another problem of interest would be the behavior of the model under periodic gust loads.

This procedure could be adapted to study of three-dimensional models by dividing the wing into segments. The feasibility of such a solution would be increased by use of the one-amplifier circuits for the unsteady forces.

REFERENCES

1. Isakson, G., <u>The Dynamic Response of an Elastic Wing to Vertical Gusts</u>,
    S. M. Thesis: Massachusetts Institute of Technology, 1947.

2. Bisplinghoff, R. L., Ashley, H., and Halfman, R. L., <u>Aeroelasticity</u>,
    Addison-Wesley, Cambridge, Mass., 1955.

3. Sears, W. R., "Some Aspects of Non-stationary Airfoil Theory and Its
    Practical Application," <u>Journal of the Aeronautical Sciences</u>, Vol. 8, No. 3,
    January 1941, page 104.

4. Fung, Y. C., <u>An Introduction to the Theory of Aeroelasticity</u>, John Wiley
    and Sons, Inc., New York, 1955.

5. Lambourne, N. C., "On the Conditions under which Energy can be Extracted
    from an Air Stream by an Oscillating Aerofoil," <u>The Aeronautical Quarterly</u>,
    Vol. IV, August 1952, pages 54-68.

Parameter	Standard Value	Range
elastic center location (fraction of chord)	.35	.25-.50
center of gravity location (fraction of chord)	.45	.30-.50
radius of gyration (fraction of chord)	.25	.20-.40
mass ratio, wing to fuselage	.333	.15-.75
standard altitude (feet)	S. L.	0-30,000
flight velocity (ft/sec.)	380	100-1200
relative density (μ)	50	
wing chord (C)	11.9	
bending stiffness parameter (K_B)	.1	
torsion stiffness parameter (K_T)	.05	

Table I. Model Parameters

Fig. 5.   Primary   Circuit   Diagram

Fig 6   Rigid Model Circuit

Fig. 7. Change of Dynamic Overstresses in Response
to Movement of the Center of Gravity or Elastic Center
from standard position

Fig. 8. Effect of Location of Center of
Gravity and Elastic Center on Frequency

Fig. 9. Effect of Location of Center of
Gravity and Elastic Center on Damping

Fig. 10. Effect of Location of Center of
Gravity and Elastic Center on Mode Shape

Fig. *11.* Effect of the Radius of

Gyration on Dynamic Overstresses

Fig. 12. Response of Frequency, Damping and
Mode Shape to Change in Radius of Gyration

35

Fig. 13. Effect of Mass Ratio on Dynamic Overstresses

Fig. 14 Effect of Mass Ratio on Frequency and Damping
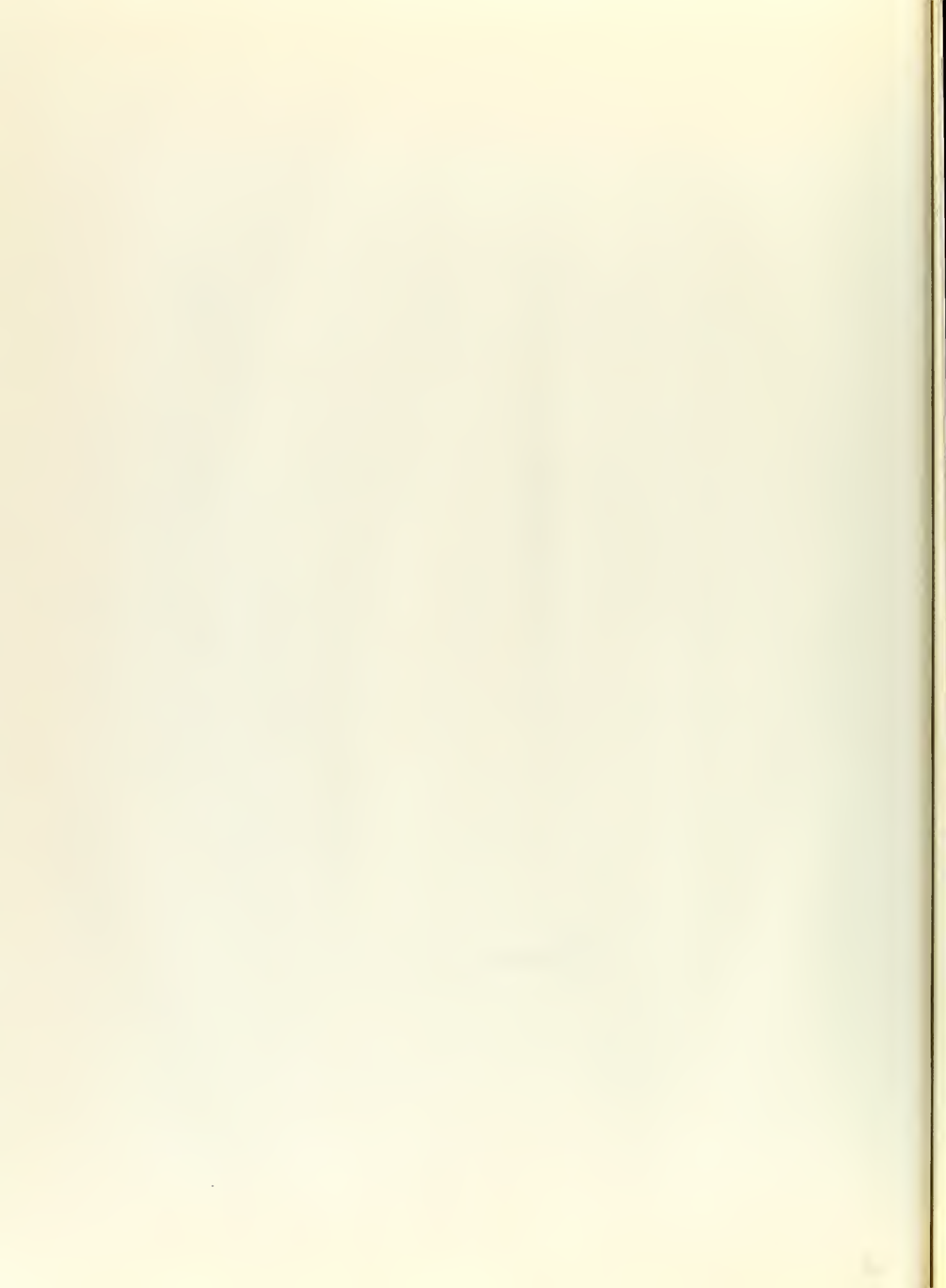
Fig. 15. Effect of Mass Ratio on Mode Shapes

Fig.16. Effect of Airspeed on Dynamic Overstresses

Fig. 17. Effect of Airspeed on Frequency and Damping

Fig. 18. Effect of Airspeed on Mode Shape

Fig. 19. Effect of Relative Density on Dynamic Overstresses

Fig 20. Effect of Altitude on Damping

Fig. 21. Effect of Gust of Finite Gradient